Current Science
CS 6 (5), 6610-6624 (2026)
Received 09 August 2026 | **Accepted 02 September** 2026 | **Online Available 03 September** 2026
https://doi.org/10.52845/CS/2026-6-5-2

Current Science

Current Science

OPEN ACCESS

ISSN (O) 2795-8639

Original Article

Circular RNA Circasap1 Facilitates Gastric Cancer Progression by Sponging Mir-874-3p and Upregulating CPEB4

Chuan Qin[1†], Lei Liu[2†], Jinkun Zhong[1*], Han Zhang[3*]

[1]Department of Gastrointestinal Surgery, Chongqing University Three Gorges Hospital, Chongqing 404000, China,

[2]Department of Hepatobiliary Surgery, Chongqing University Three Gorges Hospital, Chongqing 404000, China

[3]Department of Oncology, Chongqing University Three Gorges Hospital, Chongqing 404000, China

[†]Chuan Qin and Lei Liu contributed equally to this work and share first authorship.

***Corresponding Author: Han Zhang, Jinkun Zhong**

Abstract:

Gastric cancer (GC) ranks as the fifth most prevalent malignancy globally and the fifth leading cause of cancer-related mortality. Although age-standardized incidence rates have declined gradually over recent decades, the absolute case burden continues to rise, driven largely by population aging and demographic growth. The clinical outlook for advanced GC remains poor, creating an urgent need to dissect the underlying molecular mechanisms. Circular RNAs (circRNAs) are established post-transcriptional regulators across multiple cancer types; however, the functional roles of most circRNAs in GC pathogenesis remain poorly characterized. In this study, we identified a significantly upregulated circRNA, hsa_circ_0008934 (designated circASAP1), in GC tissues and cell lines through microarray profiling and qRT-PCR validation. Functional assays demonstrated that circASAP1 knockdown markedly suppressed, while its overexpression promoted, GC cell proliferation, colony formation, DNA synthesis, migration, and invasion in vitro. Mechanistically, circASAP1 acts as a competitive endogenous RNA (ceRNA) by directly sponging miR-874-3p, thereby derepressing the oncogenic target CPEB4. Luciferase reporter and RNA fluorescence in situ hybridization (FISH) assays confirmed the direct interactions among circASAP1, miR-874-3p, and the CPEB4 3′ untranslated region. Rescue experiments validated that the pro-tumorigenic effects of circASAP1 are mediated, at least in part, through the miR-874-3p/CPEB4 axis. These findings establish the circASAP1/miR-874-3p/CPEB4 regulatory cascade as a driver of GC progression and identify circASAP1 as a candidate prognostic biomarker and therapeutic target.

Keywords: Gastric cancer, circASAP1 (hsa_circ_0008934), miR-874-3p, CPEB4, Competing endogenous RNA (ceRNA)

Introduction

Gastric cancer (GC) remains a formidable global health challenge, ranking fifth in both incidence and cancer-related mortality worldwide. Although the age-standardized incidence rate has shown a slow downward trend in recent decades, the absolute number of GC cases continues to increase owing to population aging and growth. Clinically, due to absent or nonspecific early symptoms and the lack of public screening awareness, more than 80% of Chinese patients with GC are diagnosed at an intermediate or advanced stage[1]. The 5-year overall survival rate of metastatic GC is lower than 10%, driven mainly by uncontrolled tumour cell proliferation, early lymph node and distant metastasis, and frequent chemotherapy resistance. Although radical total gastrectomy, platinum-based

chemotherapy, anti-HER2 targeted therapy, and immune checkpoint blockade have improved clinical management, treatment outcomes for aggressive advanced GC remain unsatisfactory[2]. Identifying the core molecular pathways governing GC proliferation and invasion is therefore a priority for discovering new diagnostic biomarkers and actionable therapeutic targets[3,4.]

Non-coding RNAs have become key post-transcriptional regulators of oncogenic signalling in digestive tract malignancies over the past decade[5,6]. Circular RNAs (circRNAs) are a unique class of covalently closed single-stranded non-coding RNAs generated by back-splicing of precursor mRNAs. Lacking a 5′ cap and 3′ poly(A) tail, circRNAs resist RNase R degradation, conferring high stability, tissue specificity, and detectability in peripheral biological fluids. High-throughput RNA sequencing and microarray analysis have confirmed that aberrant circRNA expression patterns are widespread in GC tissues, peripheral exosomes, and cell lines[7]. These circRNAs regulate multiple malignant phenotypes, including cell cycle progression, epithelial–mesenchymal transition (EMT), glycolytic reprogramming, stem cell maintenance, and metastatic colonization. Beyond co-transcriptional regulation and RNA–protein scaffold functions, the most extensively characterized mechanism of circRNA action in GC is the competitive endogenous RNA (ceRNA) sponge mechanism. MicroRNAs (miRNAs) are ~22-nucleotide non-coding RNAs that suppress gene translation or trigger mRNA degradation by base-pairing with complementary miRNA response elements (MREs) in the 3′ untranslated region (3′-UTR) of target mRNAs. circRNAs are enriched in conserved MREs and can competitively sequester tumour-suppressive or oncogenic miRNAs, thereby relieving miRNA-mediated translational repression on downstream protein-coding targets and reshaping the oncogenic transcriptional program at the post-transcriptional level[8,9].

Multiple studies published in 2025–2026 have confirmed the pathological significance of the circRNA–miRNA–mRNA ternary axis in GC progression. Oncogenic circRNAs typically relieve suppression of genes that drive proliferation and invasion by sequestering tumour-suppressive miRNAs: hsa_circ_0002473 binds miR-873-5p to enhance TEAD1 expression and promotes GC cell growth and migration[10]; circ-Malat1 (circ_0002082) binds miR-154-5p, upregulating the cell cycle gene CCND2 and enhancing GC cell proliferation[11]. Conversely, downregulated tumour-suppressive circRNAs in GC can bind oncogenic miRNAs to restore expression of anti-proliferative and anti-metastatic genes: circRAB31, by sponging miR-885-5p, activates the PTEN/PI3K/AKT pathway and inhibits malignant GC progression[12]. Metabolic and microenvironmental axes further expand this network: circDNMT1 neutralizes miR-576-3p to stabilize HIF-1α and enhance hypoxic glycolysis[13], while exosome-carried circ_0006718 adsorbs miR-561-3p, upregulates SAAL1, remodels the GC stroma, and promotes invasive growth[14]. Collectively, the ceRNA network centred on circRNAs constitutes a critical regulatory layer governing the proliferative and invasive phenotype of GC.

Here, we analysed microarray data and identified a novel circRNA, hsa_circ_0008934 (designated circASAP1), which is upregulated in GC tissues and four GC cell lines. We demonstrate that circASAP1 exerts a pro-oncogenic effect on GC cell lines in vitro. Based on circASAP1, we constructed a ceRNA network and confirmed that circASAP1 binds miR-874-3p, thereby upregulating CPEB4 expression and promoting GC cell proliferation, invasion, and metastasis. Characterization of the circASAP1/miR-874-3p/CPEB4 axis provides mechanistic insight into GC development and identifies circASAP1 as a candidate target for early diagnosis and therapeutic intervention.

Materials and Methods

Clinical Specimens

From 2022 to 2023, we obtained 30 pairs of GC tissues and adjacent normal tissues from the Gastrointestinal Surgery Department of Chongqing University Affiliated Three Gorges Hospital. All patients had not received preoperative chemotherapy or radiotherapy. Tissue samples were immediately stored at −80 °C after surgery and verified by two independent pathologists. This study was approved by the Ethics Committee of Chongqing University Affiliated Three Gorges Hospital in compliance with relevant guidelines (approval no. 2021-26). All patients provided signed informed consent.

Cell Culture

Human GC cell lines (AGS, MGC-803, BGC-823, and MKN-45), the human gastric epithelial cell line GES-1, and HEK293T cells were obtained from the Cell Bank of the Chinese Academy of Sciences (Beijing, China). Cells were maintained at 37 °C in 5% CO_2 in RPMI 1640 medium (VivaCell, Shanghai, China) or DMEM (Gibco, Carlsbad, USA) supplemented with 10% fetal bovine serum (FBS; VivaCell, Shanghai, China).

Circular RNA Microarray Analysis

Microarray analysis used five pairs of fresh GC and adjacent non-cancer tissue samples, prepared by CapitalBio Technology (Beijing, China). Total RNA was extracted with TRIzol (Invitrogen, California, USA), followed by RNase R digestion (Epicenter; Illumina, California, USA) to enrich circular RNA. Enriched circRNA was amplified and transcribed into fluorescent cDNA. Hybridization was performed on an Agilent G2545A instrument. Arrays were scanned with an Agilent G2565A Microarray Scanner, raw data were collected with Agilent Feature Extraction software (v10.7), and normalized with Agilent GeneSpring (Agilent Technologies, California, USA).

RNA Extraction and qRT-PCR

Total RNA was extracted with TRIzol (TaKaRa, Japan) per manufacturer's instructions. cDNA was synthesized using the PrimeScript RT kit (RR037A; TaKaRa Bio) or a miRNA reverse-transcription kit (RiboBio). Quantitative real-time PCR was performed with TB Green Premix Ex Taq II (RR820A; TaKaRa Bio). circASAP1-specific primers were designed by GeneSeed (Guangzhou, China); remaining primers were purchased from Sangon Biotech (Shanghai, China). Primer sequences are listed in Table 1. Relative expression was calculated by the $2^{-\Delta\Delta CT}$ method.

Table 1. Quantitative real-time PCR primer sequences

Name	Primer	
CircASAP1	F:CCATCTCACATGCCACATAC	R:CGCAATCTCAGCTCCTGTTA
GAPDH	F:TTTGGTATCGTGGAAGGACTC	R:GTAGAGGCAGGGATGATGTTCT
CPEB4	F:TGGGGATCAGCCTCTTCATA	R:CAATCCGCCTACAAACACCT
AQP3	F:TGTCACTCTGGGCATCCTCATC	R:AAGCTGGTTGTCGGCGAAGT
ATXN1	F:TGGAGGCCTATTCCACTCTC	R:AATGTGGACGTACTGGTTCTG
CRCP	F:TGTGACTGCTGTGGAGATCCAG	R:ATGCTGGTGACGGTGTGGAGAA
ESR1	F:GCTTACTGACCAACCTGGCAGA	R:GGATCTCTAGCCAGGCACATTC
NUFIP2	F:AGCACCAGGAAACGCCGAAGAA	R:CTTGCTGGTTGCCATTGAGGAC
TFAP2B	F:CGAAATGGCTCTGGTATGGC	R:GCTGAGGTTGGTGATGGTGT

Plasmid Construction and Oligonucleotide Transfection

Full-length hsa_circ_0008934 was amplified by PCR and seamlessly cloned into the pLC5-ciR vector to establish a cell line stably expressing circASAP1. This was carried out by Guangzhou Jisi Biotechnology Co., Ltd., which also designed specific si-circASAP1 and a negative-control siRNA (si-NC). siRNA transfection used the RiboFECT™ CP kit (RiboBio, Guangzhou, China) per manufacturer's instructions. Knockdown and overexpression efficiency of circASAP1 were verified by qRT-PCR. Plasmid transfection used Lipofectamine 2000 (Invitrogen, Carlsbad, USA) per manufacturer's instructions. siRNA, miRNA mimic, and miRNA inhibitor sequences are listed in Table 2.

Fluorescence in Situ Hybridization (FISH) Assay

Cy3-labeled circASAP1 and Cy5-labeled miR-874-3p probes (GenePharma) were detected using a FISH kit (RiboBio). Probes were hybridized overnight; nuclei were counterstained with DAPI. Images were captured with an LSM800 laser scanning confocal microscope (Carl Zeiss Microscopy, Jena, Germany). Probe sequences are listed in Table 2.

Table 2. Nucleotide sequences of siRNA and probes

Name	Sequences
si-circASAP1-1	CUCACAUGCCACAUACAAA(dT)(dT)

si-circASAP1-2	UCACAUGCCACAUACAAAA(dT)(dT)
si-circASAP1-3	GCCACAUACAAAAAUUGAG(dT)(dT)
miR-874-3p mimics	CUGCCCUGGCCCGAGGGACCGA
miR-136-5p mimics	ACUCCAUUUGUUUUGAUGAUGGA
mimic-NC	CUGAGGGUGCCCACCGCCCGAG
inhibitor	UCGGUCCCUCGGGCCAGGGCAG
FISH probe of circASAP1	TTTTTGTATGTGGCATGTGAGAT
FISH probe of miR-874-3P	TCGGTCCCTCGGGCCAGGGCAG

Cell Proliferation and Colony Formation Assay

Transfected GC cells (2×10^3 per well) were seeded in 96-well plates and cultured for 0, 24, 48, and 72 h. Cell viability was assessed by adding 10 μL CCK-8 reagent (MedChemExpress, New Jersey, USA) for 2 h and reading absorbance at 450 nm. For colony formation, transfected cells (6×10^2 per well) were seeded in 6-well plates and cultured for 8 days, then fixed with paraformaldehyde (Servicebio, Wuhan, China) and stained with crystal violet (0.1%) (Solarbio, Beijing, China). Colonies were imaged with a CanoScan 9000F Mark II scanner (Canon, Tokyo, Japan).

5-Ethynyl-2′-deoxyuridine (EdU) Incorporation Assay

Transfected GC cells (2×10^3 per well) were seeded in 96-well plates and grown to logarithmic phase. EdU incorporation was assessed with the 5-ethynyl-2′-deoxyuridine (EdU) labelling/detection kit (RiboBio) per manufacturer's instructions: cells were fixed with 4% formaldehyde, permeabilized with 0.5% Triton X-100, and stained sequentially with Apollo solution and Hoechst 33342. Images were acquired on an LSM800 confocal microscope (Carl Zeiss, Germany).

Migration and Invasion Assays

Transfected GC cells (5×10^5) were seeded into the upper chamber of Transwell inserts (Corning, New York, USA) in 300 μL of serum-free medium for migration assays, or into chambers pre-coated with 100 μL of 1 mg/mL Matrigel (BD Biosciences, San Jose, USA) for invasion assays. The lower chamber contained 700 μL of 10% FBS medium. After 24 h, cells were fixed with paraformaldehyde (Servicebio, Wuhan, China) and stained with crystal violet (0.1%), and imaged with an inverted microscope (Leica).

Dual-luciferase Reporter Assay

Wild-type (WT) or mutant (MUT) reporter plasmids harbouring the circASAP1 sequence or the CPEB4 3′-UTR (pGL3-Firefly_Luciferase-Renilla_Luciferase) were designed and constructed by Gene Create (Wuhan, China). Plasmids were co-transfected with miR-874-3p mimic, miR-136-5p mimic, or miR-NC into HEK293T cells using Lipofectamine 2000. After 48 h, luciferase activity was measured with the dual-luciferase assay kit (Beyotime, China).

Statistical analysis

Data were analysed using GraphPad Prism (v7; https://www.graphpad.com/). Group comparisons used Student's two-tailed t-test or one-way ANOVA. Heatmaps were generated with the 'pheatmap' R package; volcano plots were generated with the 'ggplot2' R package; Venn diagrams were drawn with the 'Venn' R package. $*p < 0.05$ and $**p < 0.01$ were considered statistically significant.

Results

Characterization and Expression of Circasap1 in GC Cells and Tissues

From the microarray dataset, we identified 485 differentially expressed circRNAs (logFC > 2, FDR-adjusted $p < 0.05$). Among them, hsa_circ_0008934 (designated circASAP1) was the most significantly upregulated circRNA (Figure 1A). To verify differential expression between GC tissues and adjacent normal tissues, we collected 30 paired samples and quantified circASAP1 by qRT-PCR (Figure 1B). circASAP1 expression was also significantly higher in the AGS and MKN-45 GC cell lines than in GES-1 gastric epithelial cells (Figure 1C). circASAP1 was consistently overexpressed across GC tissues and cell lines relative to normal controls. Sanger sequencing confirmed the circular structure of circASAP1 formed by back-splicing (Figure 1D). The reverse-transcription efficiency of circASAP1 was markedly lower with oligo(dT) primers than with

random hexamers, further confirming its circular topology (Figure 1E). FISH analysis showed that circASAP1 was present in both the cytoplasm and nucleus of AGS and MKN-45 cells (Figure 1F). circASAP1 expression level showed no significant correlation with patient sex, age, differentiation grade, or tumour stage, but correlated closely with tumour size and lymph node metastasis (Table 3). On this basis, circASAP1 was selected for further study.

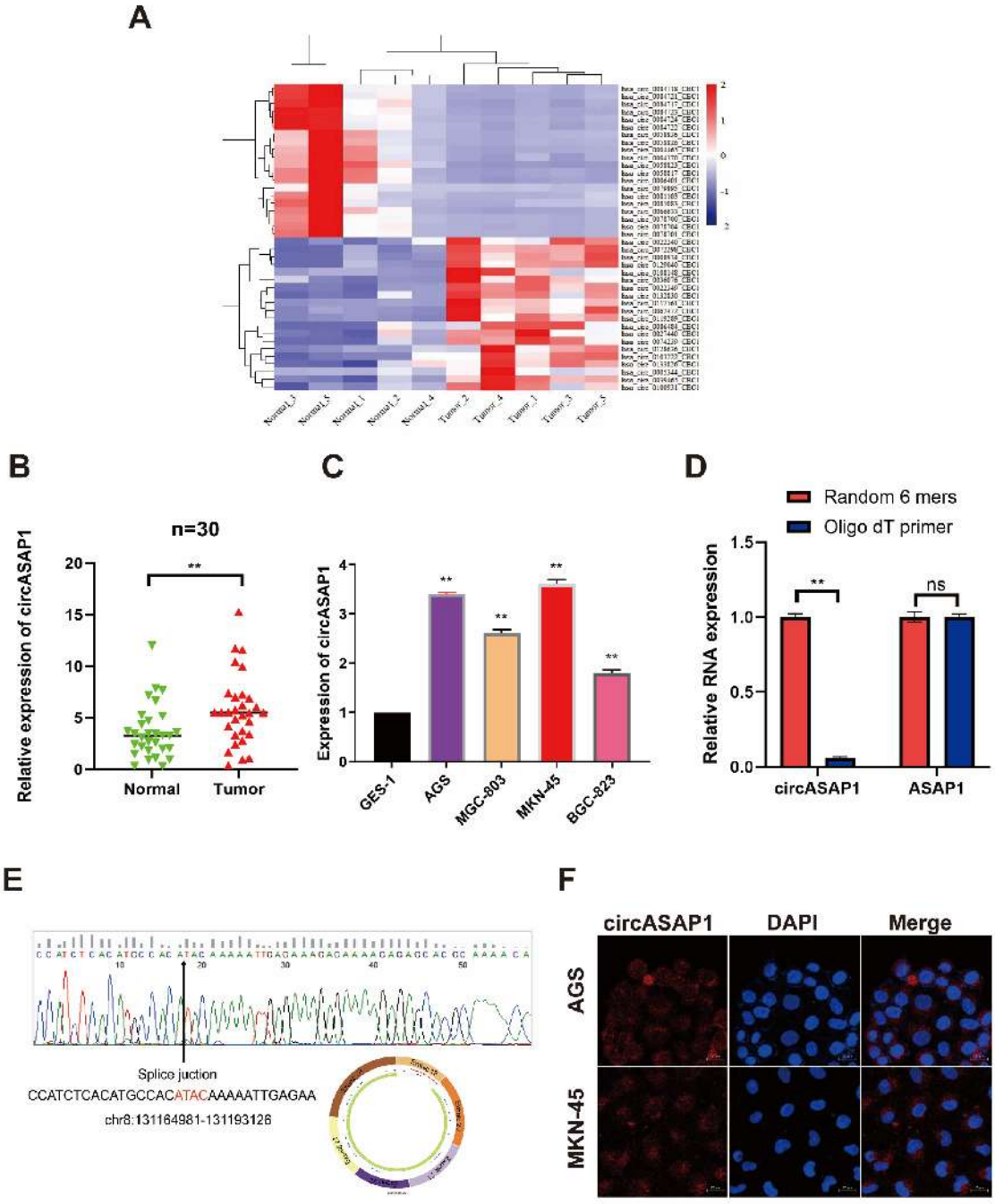

Figure 1. Characterization and expression of circASAP1 in GC cells and tissues. (A) Heatmap showing the top 20 upregulated and downregulated differentially expressed circRNAs ($p < 0.005$). (B) circASAP1 expression was upregulated in 30 GC tissues compared with adjacent normal tissues. (C) Expression of circASAP1 in GC cell lines and GES-1 cells. (D) Sanger sequencing confirmed the back-splicing junction and genomic origin of circASAP1. (E) Expression of circASAP1 and linear ASAP1 mRNA in GC cells using oligo(dT) and random hexamer primers. (F) FISH analysis showing

cytoplasmic and nuclear localization of circASAP1 in GC cells; scale bar, 20 μm. Values are mean ± SEM of three independent experiments. *$p < 0.05$ and **$p < 0.01$.

Table 3. Correlations between circASAP1 expression and clinicopathologic characteristics in GC patients

Characteristic	CircASAP1			
	All (30)	High (%) $n = 23$	Low (%) $n = 7$	p value
Gender				0.0837
Male	18	16 (69.6%)	2 (28.6%)	
Female	12	7 (30.4%)	5 (71.4%)	
Age				0.545
≥60	11	8 (34.8%)	3 (42.9%)	
<60	19	15 (65.2%)	4 (57.1%)	
Differentiation				0.068
Good	11	6 (26.1%)	5 (71.4%)	
Poor	19	17 (73.9%)	2 (28.6%)	
Tumour size				0.0139
≥50 mm	21	19 (82.6%)	2 (28.6%)	
<50 mm	9	4 (17.4%)	5 (71.4%)	
Lymph node				0.0067
N0	8	3 (13.0%)	5 (71.4%)	
N1–N3	22	20 (87.0%)	2 (28.6%)	
Stages				0.308
I–II	7	4 (17.4%)	3 (42.9%)	
III–IV	23	19 (82.6%)	4 (57.1%)	
*$p < 0.05$				

Circasap1 Knockdown Inhibits Proliferation, Colony Formation, DNA Synthesis, Migration, and Invasion of GC Cells

To determine whether circASAP1 influences GC cell biology, we designed siRNA targeting circASAP1. Knockdown efficiency of si-circASAP1 in AGS and MKN-45 cells were confirmed by qRT-PCR (Figures 2A and 2B). CCK-8 assays showed that si-circASAP1 transfection significantly reduced the proliferation of AGS and MKN-45 cells compared with si-NC controls (Figures 2C and 2D). Colony formation assays showed that AGS and MKN-45 cells transfected with si-circASAP1 formed fewer and smaller colonies (Figures 2E and 2F). EdU incorporation confirmed that circASAP1 silencing significantly reduced DNA synthesis in AGS and MKN-45 cells (Figures 2G–2I). Transwell assays demonstrated that circASAP1 knockdown inhibited migration of both AGS and MKN-45 cells and invasion of AGS cells. In MKN-45 cells, which are semi-suspension cells, the invasion assay did not yield reliable results due to the cell line's inherent growth characteristics (Figures 2J–2M).

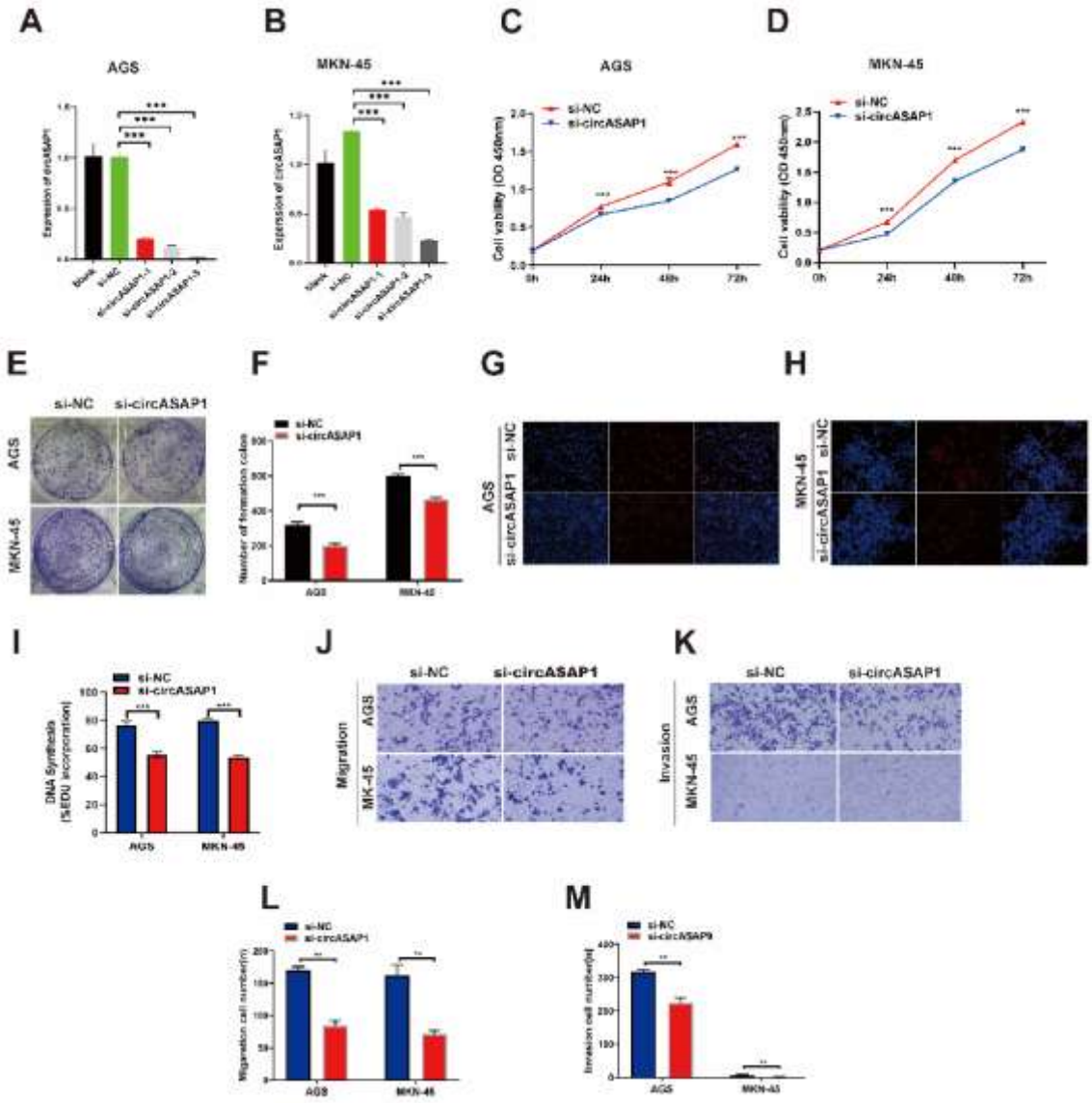

Figure 2. circASAP1 knockdown inhibits proliferation, colony formation, DNA synthesis, migration, and invasion in AGS and MKN-45 cells. (A, B) Knockdown efficiency of si-circASAP1 in AGS and MKN-45 cells. (C, D) CCK-8 assay in AGS and MKN-45 cells transfected with si-NC or si-circASAP1. (E, F) Colony formation assay in AGS and MKN-45 cells transfected with si-NC or si-circASAP1. (G–I) EdU assay in AGS and MKN-45 cells transfected with si-NC or si-circASAP1. (J, L) Migration assays in AGS and MKN-45 cells; (K) invasion assays in AGS cells. Invasion data for MKN-45 were not obtainable due to the semi-suspension phenotype of this cell line. Values are mean ± SEM of three independent experiments. **$p < 0.01$ and ***$p < 0.001$.

Circasap1 Overexpression Promotes Proliferation, Colony Formation, DNA Synthesis, Migration, and Invasion of GC Cells

Given that circASAP1 is overexpressed in GC cell lines relative to GES-1, we generated stable AGS and MKN-45 cell lines overexpressing circASAP1 and examined the functional consequences. Overexpression efficiency in AGS and MKN-45 cells was confirmed by qRT-PCR (Figures 3A and 3B). CCK-8 assays showed that circASAP1-overexpressing AGS and MKN-45 cells proliferated faster than empty-vector (NC) controls (Figures 3C and 3D). Colony formation assays revealed that circASAP1 overexpression increased colony number and size (Figures 3E and 3F). EdU incorporation showed that DNA synthesis was enhanced in circASAP1-overexpressing AGS and MKN-45 cells (Figures 3G–3I). Transwell assays confirmed that circASAP1 overexpression

promoted migration in AGS and MKN-45 cells and invasion in AGS cells. As before, reliable invasion data could not be obtained for MKN-45 cells owing to their semi-suspension character (Figures 3J–3M).

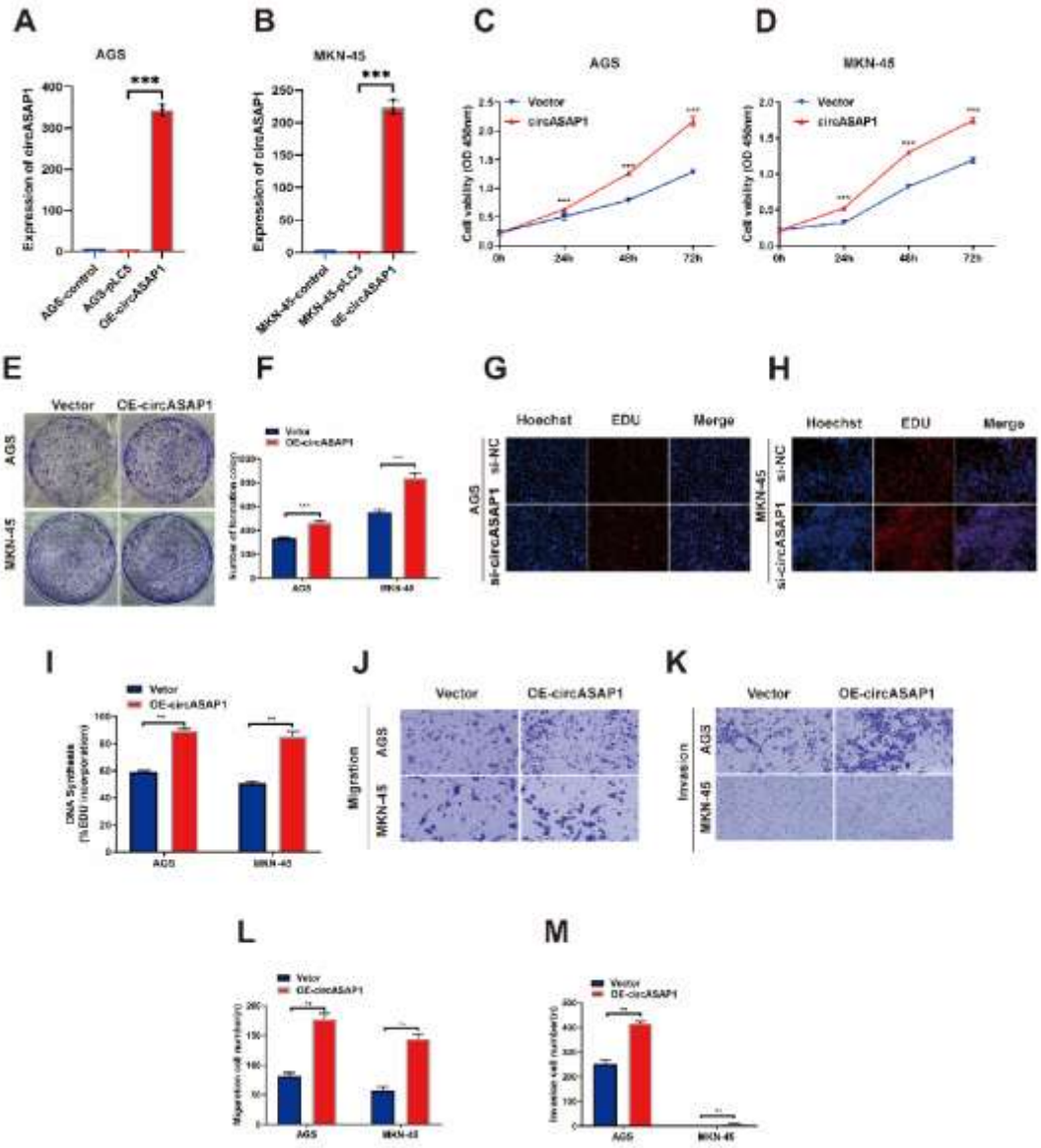

Figure 3. circASAP1 overexpression promotes proliferation, colony formation, DNA synthesis, migration, and invasion in AGS and MKN-45 cells. (A, B) Overexpression efficiency of circASAP1 in AGS and MKN-45 cells. (C, D) CCK-8 assay. (E, F) Colony formation assay. (G–I) EdU assay. (J, L) Migration assays in AGS and MKN-45 cells; (K) invasion assays in AGS cells. Invasion data for MKN-45 were not obtainable due to the semi-suspension phenotype of this cell line. Values are mean ± SEM of three independent experiments. **$p < 0.01$ and ***$p < 0.001$.

Circasap1 Directly Sponges Mir-874-3p

Bioinformatics prediction (miRDB, miRTarBase, and TargetScan) identified two candidate miRNAs that could be sponged by circASAP1: miR-874-3p and miR-136-5p. To determine whether circASAP1 interacts with these miRNAs, we constructed luciferase plasmids harbouring wild-type (WT) and mutant (MUT) circASAP1 sequences (Figure 4A). Luciferase reporter assays showed that miR-874-3p mimics significantly reduced luciferase activity of circASAP1-WT, but not circASAP1-MUT, in AGS and HEK293T cells (Figures 4B and 4C). miR-136-5p mimics had no effect on circASAP1-WT luciferase activity (Figure 4D). FISH analysis confirmed co-localization of circASAP1 and miR-874-3p in the cytoplasm of AGS and MKN-45 cells (Figure 4E). These results indicate that circASAP1

specifically sponges miR-874-3p and thereby modulates downstream GC cell behaviour.

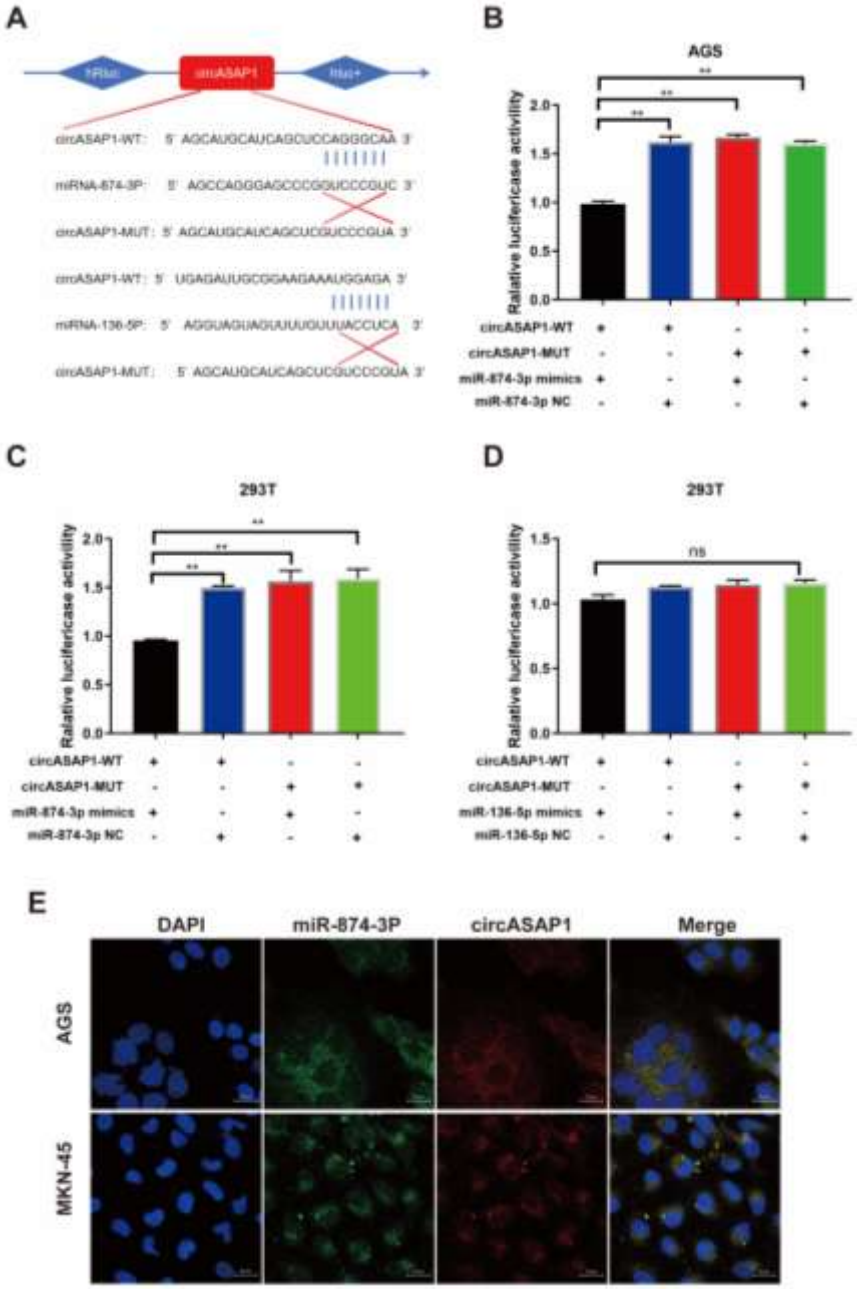

Figure 4. circASAP1 directly sponges miR-874-3p. (A) Schematic of predicted miR-874-3p and miR-136-5p binding sites in WT and MUT circASAP1. (B, C) Luciferase reporter assays confirming circASAP1–miR-874-3p interaction in (B) AGS and (C) HEK293T cells. (D) Luciferase assay showing no interaction between circASAP1 and miR-136-5p in AGS cells. (E) FISH analysis of circASAP1 and miR-874-3p co-localization in AGS and MKN-45 cells; scale bar, 20 µm. Values are mean ± SEM of three independent experiments. *$p < 0.05$ and **$p < 0.01$.

Circasap1 Overexpression Reverses the Tumour-Suppressive Effects of Mir-874-3p on GC Cell Proliferation and Invasion

To determine whether miR-874-3p mediates the functional changes driven by circASAP1, we co-transfected circASAP1 and miR-874-3p mimics into AGS and MKN-45 cells. miR-874-3p mimics significantly reduced proliferation of both cell lines, while co-expression of circASAP1 rescued this suppression (Figures 5A–5D). Similarly, circASAP1 restored DNA synthesis suppressed by miR-874-3p (Figures 5E and 5F). In migration and invasion assays, exogenous miR-874-3p reduced

motility and invasiveness of GC cells; circASAP1 co-transfection partially reversed the reduction in migration in AGS and MKN-45 cells (Figures 5G and 5I) and the reduction in AGS cell invasion (Figure 5H). In MKN-45 cells, invasion results remained unreliable due to the semi-suspension phenotype (Figure 5J).

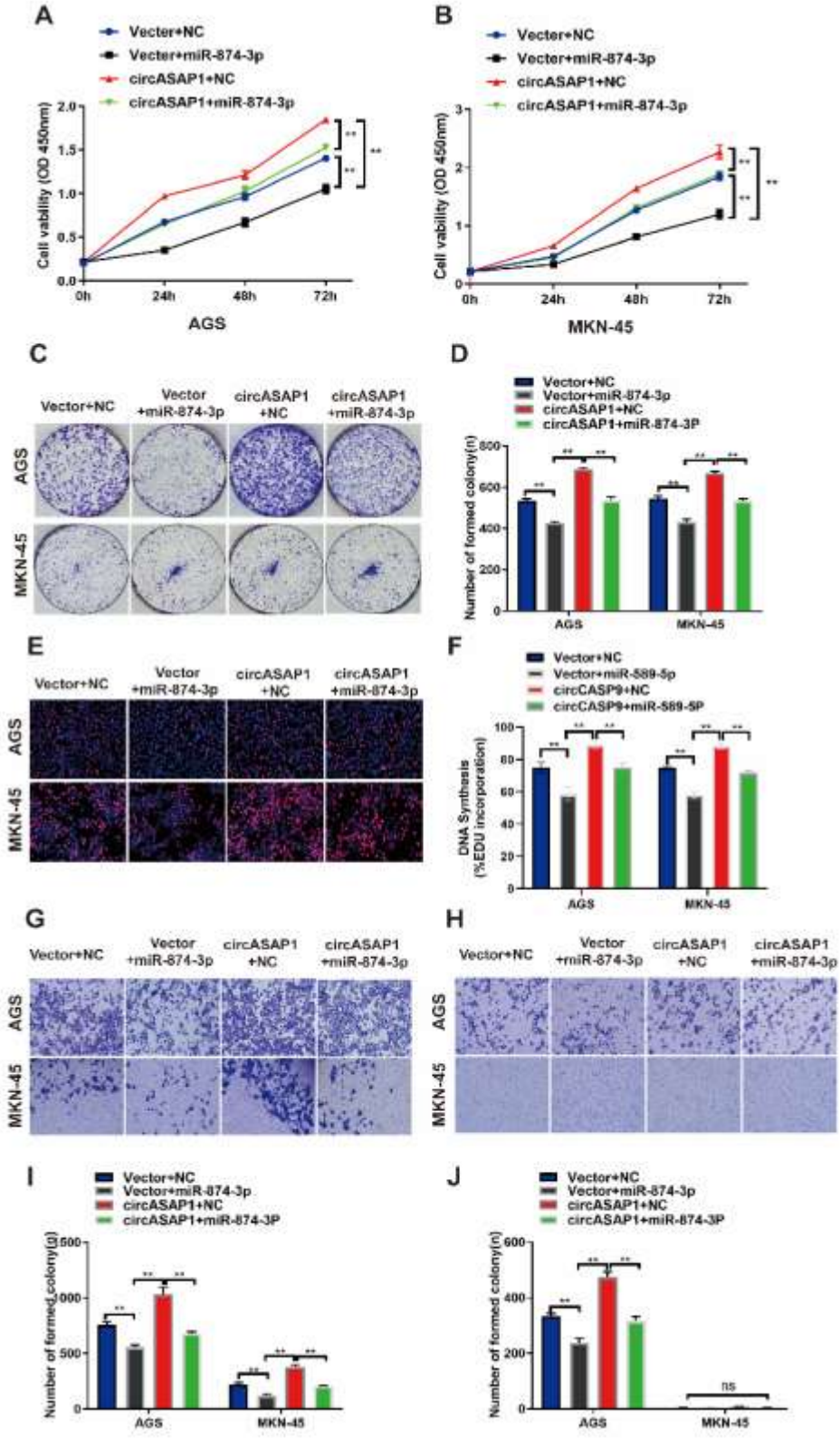

Figure 5. circASAP1 overexpression reverses the tumour-suppressive effects of miR-874-3p on GC cell proliferation and invasion. (A, B) CCK-8 assay of AGS and MKN-45 cells co-transfected with miR-874-3p mimics and circASAP1. (C, D) Colony formation assay. (E, F) EdU assay. (G, I)

Migration assays in AGS and MKN-45 cells; (H, J) Invasion assays in AGS cells. Invasion data for MKN-45 were not obtainable due to the semi-suspension phenotype of this cell line. Values are mean ± SEM of three independent experiments. *$p < 0.05$ and **$p < 0.01$.

The circASAP1/miR-874-3p axis directly regulates CPEB4 in GC cells

circASAP1 sequesters miR-874-3p, affecting proliferation, migration, and invasion of GC cells. To identify the downstream mediator, we screened the expression of seven candidate GC-related genes predicted as miR-874-3p targets (ATXN1, AQP3, CPEB4, CRCP, ESR1, NUFP2, TFAP2B) by qRT-PCR (Figure 6A). Knockdown of circASAP1 in AGS and MKN-45 cells consistently reduced CPEB4 mRNA levels, suggesting that the circASAP1/miR-874-3p axis regulates GC behaviour through CPEB4 (Figures 6B and 6C). To confirm CPEB4 as a direct miR-874-3p target, we generated luciferase reporters harbouring the WT or MUT (miR-874-3p binding site deleted) CPEB4 3′-UTR (Figure 6D). In HEK293T and AGS cells, miR-874-3p mimics significantly suppressed luciferase activity driven by CPEB4 3′-UTR-WT but not CPEB4 3′-UTR-MUT (Figures 6E and 6F). These data confirm that circASAP1 promotes GC cell proliferation and invasion by sponging miR-874-3p and thereby derepressing CPEB4 expression.

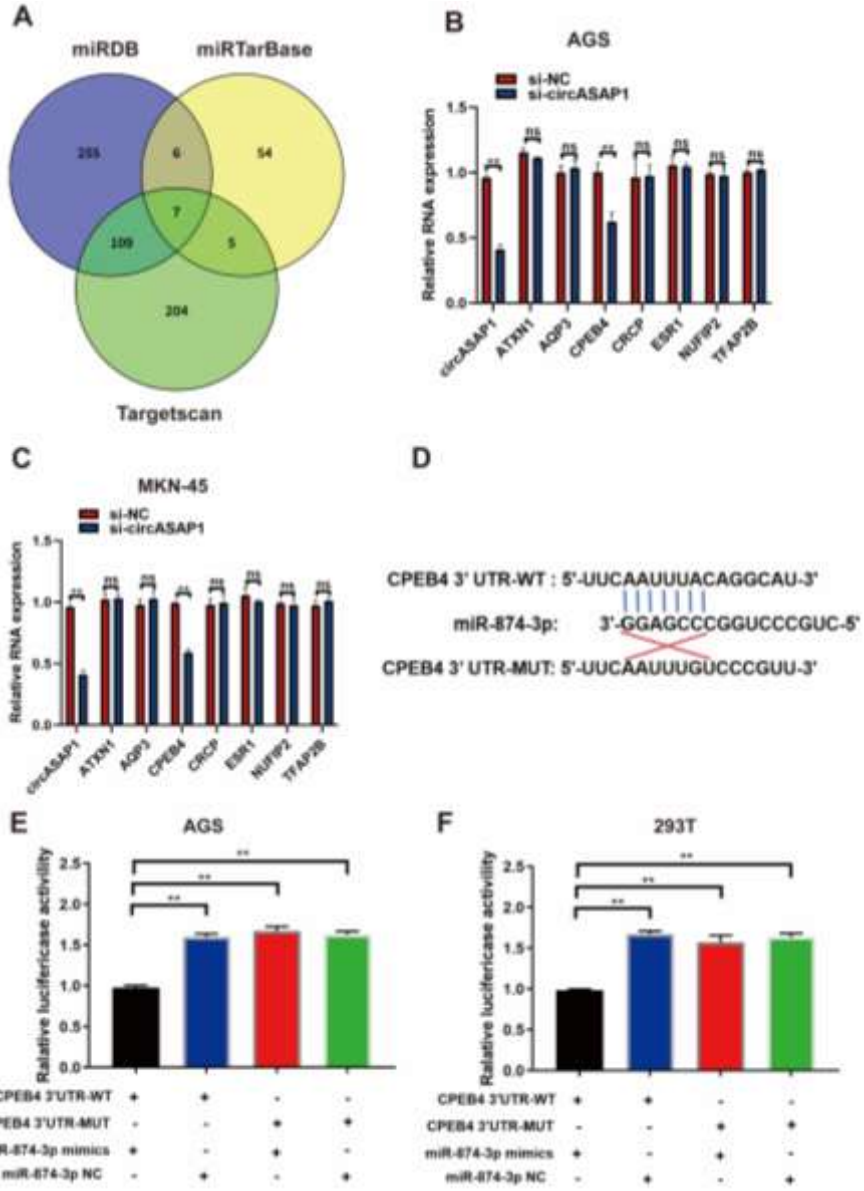

Figure 6. CPEB4 is a downstream target of the circASAP1/miR-874-3p axis. (A) Bioinformatics prediction of miR-874-3p target genes using miRDB, miRTarBase, and TargetScan. (B, C) CPEB4

mRNA expression after circASAP1 knockdown in AGS and MKN-45 cells. (D) Schematic of predicted miR-874-3p binding site in WT and MUT CPEB4 3′-UTR. (E, F) Dual-luciferase reporter assays confirming miR-874-3p–CPEB4 interaction in AGS and HEK293T cells. Values are mean ± SEM of three independent experiments. *p < 0.05 and **p < 0.01.

Discussion

The ceRNA hypothesis, first articulated by Salmena *et al.*[15], proposes that transcripts sharing common MREs compete for miRNA binding and thereby co-regulate one another's expression. This paradigm has reshaped the conceptual framework of gene regulation, positioning non-coding RNAs—particularly circRNAs—as active participants in post-transcriptional regulatory networks. Among all functional mechanisms attributed to circRNAs, the miRNA sponge model remains the most extensively studied[16]. CircRNAs are especially well-suited to this role: their covalently closed structure, generated by back-splicing (in which a downstream 5′ splice donor joins an upstream 3′ splice acceptor), renders them highly resistant to exonucleolytic degradation. This confers longer half-lives and greater expression stability than linear RNAs, allowing circRNAs to accumulate numerous miRNA-binding sites and effectively sequester miRNAs in cells. This structural advantage is particularly relevant in the nuclease-rich tumour microenvironment[17]. CircRNA-mediated miRNA sponging has broad functional significance across cancer types. In GC, multiple circRNAs have been identified as components of ceRNA networks that modulate critical signalling pathways[18,19]. For example, circZFAND6 suppresses GC metastasis via the miR-6815-3p/APC/Wnt-β-catenin pathway[20], while circNRIP1 promotes GC progression by sponging miR-149-5p and activating the AKT1/mTOR pathway[21]. Comprehensive circRNA–miRNA–mRNA ceRNA networks reveal that dysregulated circRNA transcripts, their miRNA targets, and downstream effector genes collectively contribute to GC pathogenesis[19]. These findings position the ceRNA axis as a core mechanism through which circRNAs exert oncogenic or tumour-suppressive functions in gastrointestinal malignancies[9].

Accumulating evidence indicates circRNA dysregulation during GC development[17,22]. This study identifies circASAP1 as a significantly upregulated circRNA in GC tissues and cell lines and characterizes its oncogenic function and underlying ceRNA mechanism. Our results show that circASAP1 promotes proliferation, clonogenicity, migration, and invasion of GC cells through the circASAP1/miR-874-3p/CPEB4 signalling pathway, providing mechanistic insight into GC progression. The aberrant overexpression of circASAP1 in GC tissues compared with matched normal mucosa aligns with the emerging view that dysregulated circRNAs drive tumorigenesis[22,23]. Gain-of-function and loss-of-function experiments consistently demonstrate that circASAP1 exerts pro-tumorigenic effects: overexpression enhances malignant phenotypes, and knockdown suppresses them. This is consistent with previous reports on oncogenic circRNAs in gastrointestinal malignancies, including circTHBS1[24], hsa_circ_0013729[25], and circRNA_0023685[26]. Notably, circASAP1 expression correlates with tumour volume and lymph node metastasis, suggesting clinical utility as a prognostic marker.

Our study demonstrates that circASAP1 acts as a ceRNA for miR-874-3p. Dual-luciferase reporter assays confirmed direct binding between circASAP1 and miR-874-3p, and the negative correlation between their expression levels in clinical samples supports a functional relationship. Rescue experiments showed that exogenous miR-874-3p partially reversed phenotypes induced by circASAP1 overexpression, and miR-874-3p inhibition partially restored malignant behaviours after circASAP1 silencing, establishing circASAP1 as an upstream regulator that relieves miR-874-3p-mediated post-transcriptional repression. miR-874-3p exerts tumour-suppressive effects across multiple cancer types[27,28]. In GC, miR-874-3p suppresses migration, invasion, and drug resistance by targeting GDPD5[27], and inhibits angiogenesis via the STAT3/VEGF-A pathway[28]. Its reduced expression in GC tissues and cell lines aligns with the view that circASAP1 overexpression sequesters this protective miRNA, relieving suppression of GC progression. This mechanism is conserved across epithelial malignancies: in endometrial cancer, circESRP1 promotes metastasis through the same miR-874-3p/CPEB4 axis[29], suggesting the miR-

874-3p/CPEB4 module has broad oncogenic significance.

Downstream of miR-874-3p, CPEB4 (cytoplasmic polyadenylation element binding protein 4) promotes GC progression through ZEB1-mediated EMT[30] and has been associated with cisplatin resistance and other aggressive GC traits[31]. By sponging miR-874-3p and thereby derepressing CPEB4, circASAP1 drives a coherent oncogenic cascade. Additionally, circASAP1 is derived from the ASAP1 locus; ASAP1 itself activates the IQGAP1/CDC42 pathway to promote GC progression and chemotherapy resistance[32], suggesting that the parent gene and its derived circRNA may cooperate in tumour promotion. Exosome-mediated delivery of circRNAs has been identified as a mechanism of intercellular communication in GC[33,34], and future work should explore whether circASAP1 is packaged into exosomes and influences the GC tumour microenvironment.

This study has several limitations. First, all functional experiments were conducted in vitro; in vivo validation using orthotopic or subcutaneous tumour models are required to confirm the oncogenic role of circASAP1. Second, the CPEB4 rescue experiment (restoring CPEB4 after circASAP1 knockdown) was not performed and should be included to formally establish CPEB4 as the functional effector of the circASAP1/miR-874-3p axis. Third, the clinical cohort (n = 30) is relatively small; validation in a larger, independent patient series is needed. Despite these limitations, our findings identify circASAP1 as a driver of GC progression through the circASAP1/miR-874-3p/CPEB4 cascade and suggest it as a candidate prognostic biomarker and therapeutic target.

Author contributions

All authors contributed to the study conception and design. Material preparation, data collection and analysis were performed by Chuan Qin, Lei Liu and Jinkun Zhong. The first draft of the manuscript was written by Han Zhang. All authors commented on previous versions of the manuscript. All authors read and approved the final manuscript.

Funding

This work was supported by the Doctoral "Fast-Track" Research Project of Wanzhou District, Chongqing (Grant numbers: wzstc20230407).

Conflicts of interest

The authors declare no conflicts of interest.

Data availability statement

The data analyzed during the current study are available from the corresponding author on reasonable request.

Ethics statement

This work was approved by the Institutional Review Board of Chongqing University Three Gorges Hospital and all the research was performed in accordance with relevant guidelines.

Informed consent statement

Informed consent was obtained from all individual participants included in the study.

References

1. Bray, F., Laversanne, M., Sung, H., Ferlay, J., Siegel, R. L., Soerjomataram, I., and Jemal, A., Global cancer statistics 2022: GLOBOCAN estimates of incidence and mortality worldwide for 36 cancers in 185 countries. *CA Cancer J. Clin.*, 2024, **74**(3), 229–263. https://doi.org/10.33 22/caac.21834
2. Mamun, T. I., Younus, S., and Rahman, M. H., Gastric cancer—Epidemiology, modifiable and non-modifiable risk factors, challenges and opportunities: An updated review. *Cancer Treat. Res. Commun.*, 2024, **41**, 100845. https://doi.org/10.1016/j.ctarc.2024.100845
3. Thrift, A. P., Wenker, T. N., and El-Serag, H. B., Global burden of gastric cancer: Epidemiological trends, risk factors, screening and prevention. *Nat. Rev. Clin. Oncol.*, 2023, **20**(5),338–349. https://doi.org/10.1038/s4157 1-023-00747-0
4. Waddell, T., Verheij, M., Allum, W., Cunningham, D., Cervantes, A., and Arnold, D., Gastric cancer: ESMO-ESSO-ESTRO clinical practice guidelines for diagnosis, treatment and follow-up. *Ann. Oncol.*, 2014, **24**(Suppl 6), vi57–vi63. https://doi.org/10.10 93/annonc/mdt344
5. Han, Z. *et al*., Non-coding RNAs in gastric cancer: Mechanisms and therapeutic prospects. *Mol. Cancer*, 2025, **24**(1), 244. https://doi.org/10.1186/s12943-025-02467-8
6. Shah, A., Non-coding RNA: Architects of cellular complexity and agents of malignancy. *Genes*, 2026, **17**(3), 304. https://doi.org/10.33

90/genes17030304
7. Jiang, Z., Peng, Y., and Yang, X., Circular RNAs in tumor biology and immunology: Molecular mechanisms and therapeutic implications. *Mol. Cancer*, 2026. https://doi.org/10.1186/s12943-026-02708-4
8. Xie, L. F., Liu, S. Y., and Dang, X. W., Recent advances of circular RNAs in gastrointestinal cancer. *World J. Clin. Oncol.*, 2025, **16**(10), 111115. https://doi.org/10.5306/wjco.v16.i10.111115
9. Bakhti, S. Z., Latifi-Navid, S., Pahlevan, A. D., Sarabi, L., and Safaralizadeh, R., The role of circular RNAs in gastric cancer: Focusing on autophagy, EMT, and their crosstalk. *Biochem. Biophys. Rep.*, 2025, **43**, 102169. https://doi.org/10.1016/j.bbrep.2025.102169.
10. Wang, M., Wu, Z., Tong, R., Geng, Y., Li, F., Huo, X., and Yu, L., Circular RNA hsa_circ_0002473 boosts gastric cancer progression via the miR-873-5p/TEAD1 axis. *Biochem. Genet.*, 2026. https://doi.org/10.1007/s10528-026-11407-0
11. Li, L., Yang, L., Wang, Y., and Nan, K., Circ-malat1 promotes gastric cell growth via miR-154-5p/CCND2. *Front. Genet.*, 2025, **16**, 1594354. https://doi.org/10.3389/fgene.2025.1594354
12. Liang, X., Qin, C., Yu, G., Guo, X., Cheng, A., Zhang, H., and Wang, Z., Circular RNA circRAB31 acts as a miR-885-5p sponge to suppress gastric cancer progression via the PTEN/PI3K/AKT pathway. *Mol. Ther. Oncolytics*, 2021, **23**, 501–514. https://doi.org/10.1016/j.omto.2021.11.002
13. Li, H. *et al.*, circDNMT1 promotes malignant progression of gastric cancer through targeting miR-576-3p/hypoxia inducible factor-1 alpha axis. *Front. Oncol.*, 2022, **12**, 817192. https://doi.org/10.3389/fonc.2022.817192
14. Zhang, F. *et al.*, Small extracellular vesicles-derived circ6718 unlocks stromal remodeling and serves as a biomarker in gastric cancer. *Adv. Sci.*, 2026. https://doi.org/10.1002/advs.202521334
15. Salmena, L., Poliseno, L., Tay, Y., Kats, L., and Pandolfi, P. P., A ceRNA hypothesis: The Rosetta Stone of a hidden RNA language? *Cell*, 2011, **146**(3), 353–358. https://doi.org/10.1016/j.cell.2011.07.014
16. Shahpari, M., Hashemi, M., Younesirad, T., Hasanzadeh, A., Mosanne, M. M., and Ahmadifard, M., The functional roles of competitive endogenous RNA (ceRNA) networks in apoptosis in human cancers: The circRNA/miRNA/mRNA regulatory axis and cell signaling pathways. *Heliyon*, 2024, **10**(21), e37089. https://doi.org/10.1016/j.heliyon.2024.e37089
17. Guha, D., Mondal, J., Nandy, A., Biswas, S., and Bagchi, A., Interplay of circular RNAs in gastric cancer—A systematic review. *Front. Syst. Biol.*, 2024,**4**,1497510. https://doi.org/10.3389/fsysb.2024.1497510
18. Xu, B. *et al.*, Comprehensive analysis of circular RNA-associated competing endogenous RNA networks and immune infiltration in gastric cancer. *Transpl. Immunol.*, 2023, **77**, 101793. https://doi.org/10.1016/j.trim.2023.101793
19. Yu, J. *et al.*, CircRNA CeRNA networks in gastric cancer highlight FAP/FNDC1 as potential prognostic and therapeutic targets. *Discov. Oncol.*, 2025, **17**(1), 129. https://doi.org/10.1007/s12672-025-04230-3
20. Deng, Z. *et al.*, CircZFAND6 suppresses gastric cancer metastasis and reduces resistance to TKI therapy. *Mol. Cancer*, 2025, **24**(1), 305. https://doi.org/10.1186/s12943-025-02478-5
21. Zhang, X. *et al.*, Circular RNA circNRIP1 acts as a microRNA-149-5p sponge to promote gastric cancer progression via the AKT1/mTOR pathway. *Mol. Cancer*, 2019, **18**(1), 20. https://doi.org/10.1186/s12943-018-0935-5
22. Han, M., Zhang, M., Qi, M., Zhou, Y., Li, F., and Fang, S., Regulatory mechanism and promising clinical application of exosomal circular RNA in gastric cancer. *Front. Oncol.*, 2023, **13**,1236679. https://doi.org/10.3389/fonc.2023.1236679
23. Xia, K., Wang, Z., Liu, B., Wang, W., Liu, Y., Tang, J., and Yan, J., Functions of circular RNAs and their potential applications in gastric cancer (Review). *Oncol. Lett.*, 2023, **25**(6), 217. https://doi.org/10.3892/ol.2023.13803
24. Qiu, S. *et al.*, CircTHBS1 drives gastric cancer progression by increasing INHBA mRNA expression and stability in a ceRNA- and RBP-dependent manner. *Cell Death Dis.*, 2022, **13**(3), 266. https://doi.org/10.1038/s41419-022-04720-0
25. Li, H., Chen, S., Zhong, Y., and Meng, L., Hsa_circ_0013729 promotes gastric cancer

progression by regulating MEF2D in ceRNA- and RBP-dependent manners. *Biochem. Genet.*, 2026, **64**(3), 3723–3741. https://doi.org/10.1007/s10528-025-11216-x

26. Zhou, Y. *et al.*, Upregulation of circRNA_0023685 promotes gastric cancer progression via a circRNA-miRNA-mRNA interaction network. *Am. J. Cancer Res.*, 2024, **14**(1), 130–144. https://doi.org/10.62347/TGBA1922
27. Zhang, X. *et al.*, MiR-874-3p represses the migration and invasion yet promotes the apoptosis and cisplatin sensitivity via being sponged by long intergenic non-coding RNA 00922 (LINC00922) and targeting Glycerophosphodiester Phosphodiesterase Domain Containing 5 (GDPD5) in gastric cancer cells. *Bioengineered*, 2022, **13**(3), 7082–7104. https://doi.org/10.1080/21655979.2022.2045831
28. Zhang, X. *et al.*, miR-874 functions as a tumor suppressor by inhibiting angiogenesis through STAT3/VEGF-A pathway in gastric cancer. *Oncotarget*, 2015, **6**(3), 1605–1617. https://doi.org/10.18632/oncotarget.2748
29. Shi, R. *et al.*, CircESRP1 enhances metastasis and epithelial–mesenchymal transition in endometrial cancer via the miR-874-3p/CPEB4 axis. *J. Transl. Med.*, 2022, **20**(1), 139. https://doi.org/10.1186/s12967-022-03334-6
30. Cao, G., Chen, D., Liu, G., Pan, Y., and Liu, Q., CPEB4 promotes growth and metastasis of gastric cancer cells via ZEB1-mediated epithelial-mesenchymal transition. *Onco Targets Ther.*, 2018, **11**, 6153–6165. Https://doi.org/10.2147/OTT.S175428
31. Fei, Y. *et al.*, Circ_0008315 promotes tumorigenesis and cisplatin resistance and acts as a nanotherapeutic target in gastric cancer. *J. Nanobiotech.*, 2024, **22**(1), 519. https://doi.org/10.1186/s12951-024-02760-6
32. Xie, W. *et al.*, ASAP1 activates the IQGAP1/CDC42 pathway to promote tumor progression and chemotherapy resistance in gastric cancer. *Cell Death Dis.*, 2023, **14**(2), 124. https://doi.org/10.1038/s41419-023-05648-9
33. Jin, Y., Wang, J., Zhang, C., Li, J., Wei, C., and Zhou, Y., Exosomal circRNAs: The key role and potential therapeutic target in gastric cancer. *Curr. Cancer Drug Targets*, 2025, **25**(11), 1349–1363. https://doi.org/10.2174/0115680096318527240909082011
34. Qian, N. *et al.*, Reprogramming of hsa_circ_0008719 and its target miR-3615 induced by TOB1 in exosomes of gastric cancer cells: A contribution to inhibit gastric cancer progression. *Sci. Rep.*, 2025, **15**(1), 27089. https://doi.org/10.1038/s41598-025-12789-8